Int. J. Solids Structures, 1968, Vol. 4, pp. 1 to 13. Pergamon Press. Printed in Great Britain

DYNAMIC REACTIONS ALONG A RIGID-SMOOTH WALL IN AN ELASTIC HALF-SPACE WITH A MOVING BOUNDARY LOAD

STEPHEN A. THAU

Department of Mechanics, Illinois Institute of Technology, Chicago, Illinois

Abstract—This paper studies the dynamic forces exerted along the sides of a rigid-smooth wall which separates an elastic half-space into two quarter-spaces. The boundary of the half-space is subjected to a pressure wave of arbitrary shape moving with constant velocity. Both the shape and velocity of the wave may change as it passes the wall. The problems for each quarter-space are analyzed exactly using the method of images in conjunction with previously established techniques for dynamic half-space problems. Explicit results for the total force and moment exerted on the wall are presented. These reactions are proportional to the convolution of the load history with unity and time, respectively. The proportionality constants are evaluated numerically over a wide range of pressure wave velocities.

1. INTRODUCTION

IN RECENT years many studies have been made on the scattering of stress waves by cavities and inclusions in elastic media with emphasis on evaluation of the dynamic response of the scattering obstacle. Some of this work is listed in the recent papers of Thau and Pao [1], who considered the interaction of shear waves with parabolic shaped cavities and inclusions, and of Mow and Workman [2], who treated the problem of a fluid filled cavity struck by a compressional wave. Other papers are reviewed in the survey article on elastic wave propagation by Miklowitz [3].

Apparently, however, all the investigations in this area have taken the elastic medium surrounding the obstacle to be infinite in extent. Therefore, for applications in design of underground structures set near the ground surface, studies on scattering of elastic waves by obstacles in a half-space should be useful; and this paper presents such a study.

The problem of scattering of elastic waves by a semi-infinite, rigid-smooth wall of finite thickness which divides a half-space into two quarter-spaces is treated (Fig. 1). The surface of the half-space is subjected to an arbitrary pressure wave moving with constant velocity. Since the rigid-smooth wall is assumed to be stationary, boundary conditions along its surfaces specify the normal displacement, u_x, and the shear stress, τ_{xy}, to vanish. Furthermore, these conditions imply that the responses in the two quarter-spaces are independent.

To solve the two quarter-space problems with rigid-smooth vertical boundaries, the method of images can be used. This is because both u_x and τ_{xy} vanish identically along the y-axis in a half-space which is loaded symmetrically about this axis. On the other hand, it is noted that for a rigid wall with "rough" surfaces (both displacements vanish) the method of images fails to provide the solution. In fact, the problem of a quarter-space with a rigid-rough vertical boundary has, so far, been too complicated to solve.

Principal results of this investigation are the normal forces exerted on each side of the wall and the moments acting at the top of the wall. The former reactions are found to be

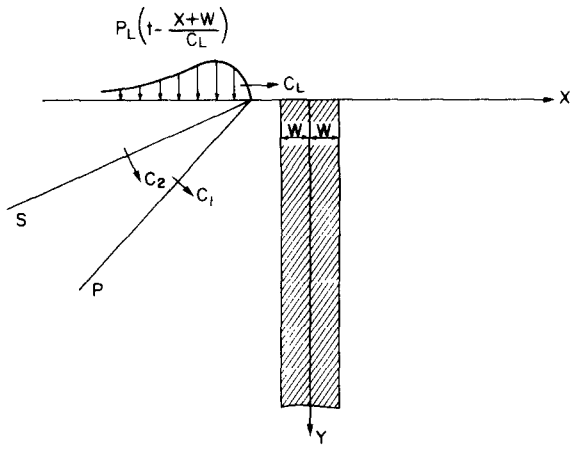

FIG. 1. Geometry of problem and incident waves.

proportional to the integral of the pressure wave load, while the moments are proportional to the convolution of the pressure wave and time. The proportionality constants are calculated for a wide range of pressure wave velocities with the Poisson's ratio of the half-space taken as 0·25.

2. MATHEMATICAL FORMULATION OF PROBLEM

Both the pressure wave load which moves along the surface of the half-space and the rigid-smooth wall imbedded within (Fig. 1) are assumed to extend indefinitely in the z-direction. Thus, the medium is taken to be in a state of plane strain in which the z-displacement is zero and the x and y displacements and stresses are independent of z. The equations of motion for the waves in the elastic quarter-spaces become:

$$c_1^2\nabla^2\phi-\ddot{\phi}=0; \qquad c_2^2\nabla^2 h-\ddot{h}=0 \tag{1}$$

where ∇^2 is the Laplacian, dots indicate time derivatives,

$$c_1=c_2/\varepsilon, \qquad c_2=(\mu/\rho) \quad \text{with} \quad \varepsilon^2=(1-2\nu)/(2-2\nu) \tag{2}$$

are the velocities of the compressional (P) and shear (S) waves, respectively, with μ, ν, and ρ being the shear modulus, Poisson's ratio, and density of the elastic medium.

The compressional wave potential, $\phi(x, y, t)$, and the shear wave potential, $h(x, y, t)$, are related to the displacements by

$$u_x=\partial\phi/\partial x+\partial h/\partial y, \qquad u_y=\partial\phi/\partial y-\partial h/\partial x \tag{3}$$

and the stresses, τ_{ij}, are determined from Hooke's Law:

$$\tau_{ij}=\mu[u_{i,j}+u_{j,i}+2\nu u_{k,k}\delta_{ij}/(1-2\nu)] \tag{4}$$

where Cartesian tensor notation is used in (4) with δ_{ij} being the Kronecker delta.

Boundary conditions along both sides of the rigid-smooth wall ($x = \pm w$) specify the normal displacement and shear stress to vanish, i.e.,

$$u_x(\pm w, y, t) = \tau_{xy}(\pm w, y, t) = 0. \tag{5}$$

To complete the mathematical formulation of the problem, boundary conditions along the surface of the half-space must be specified. First, however, we shall discuss the assumptions which are made concerning the pressure wave loading.

The load is taken to occur originally far to the left of the wall ($x \to -\infty$) and it travels in the positive x-direction with constant velocity. The instant its front reaches the left side of the wall ($x = -w$) is taken as $t = 0$; the time it reaches the right side is $t = t_0$ where, of course, t_0 depends on the wall thickness, $2w$. In progressing from the left to the right side of the wall, both the velocity and intensity of the load are permitted to change. We shall denote the velocity and variable intensity along the left quarter-space by c_L and $p_L(t)$, respectively, and similarly along the right side by c_R and $p_R(t)$. It is understood that $p_L[t-(x+w)/c_L] \equiv 0$ for $t < (x+w)/c_L$ and $p_R[t-(x-w)/c_R] \equiv 0$ for $t < (x-w)/c_R$.

The velocity of the load along the left-hand quarter-space, c_L, is supersonic (i.e., c_L is greater than the elastic wave speeds) so that the elastic waves strike the left side of the wall initially at $t = 0$. Note that for pressure wave velocities less than the elastic wave velocities, the problem for the left quarter-space would be indeterminate because disturbances propagating therein would strike the wall at some indefinite time before the pressure wave reaches the wall. One would have to specify a finite time and position for the origin of the load in order to consider transonic ($c_2 < c_L < c_1$) and subsonic ($c_L < c_2$) load velocities over the left-hand quarter-space. On the other hand, since the inception of loading of the right-hand quarter-space occurs at a definite position ($x = w$) and time ($t = t_0$), we can consider the constant velocity of the load thereupon, c_R, to be arbitrary.

Now, the remaining boundary conditions become:

$$\tau_{yy}(x, 0, t) = -p_L(t-x/c_L-w/c_L); \qquad x < -w, -\infty < t < \infty \tag{6a}$$

$$\tau_{yy}(x, 0, t) = \begin{cases} 0; & x > w, t < t_0 \\ -p_R(t-t_0-x/c_R+w/c_R); & x > w, t > t_0 \end{cases} \tag{6b}$$

$$\tau_{xy}(x, 0, t) = 0; \qquad -\infty < x < \infty, -\infty < t < \infty \tag{6c}$$

As the above conditions imply, the problems for the left and right-hand quarter-spaces can be treated separately. This is done in the following section.

3. SOLUTION OF PROBLEM AND REACTIONS ON WALL

Mathematically, the problem in each quarter-space is to solve the equations of dynamic elasticity for plane strain, equations (1)–(4), subject to the boundary conditions (5) and (6). As explained in the introduction, boundary conditions (5) are satisfied identically along the y-axis in a half-space with symmetric loading about this axis (Figs. 2 and 3). Hence, the responses in the left and right-hand quarter-spaces in Fig. 1 can be determined from the responses in the left half of the half-spaces in Figs. 2 and in the right half of the half-space in Fig. 3, respectively, with

$$x_L = x+w, \qquad x_R = x-w, \qquad y_L = y_R = y \tag{7}$$

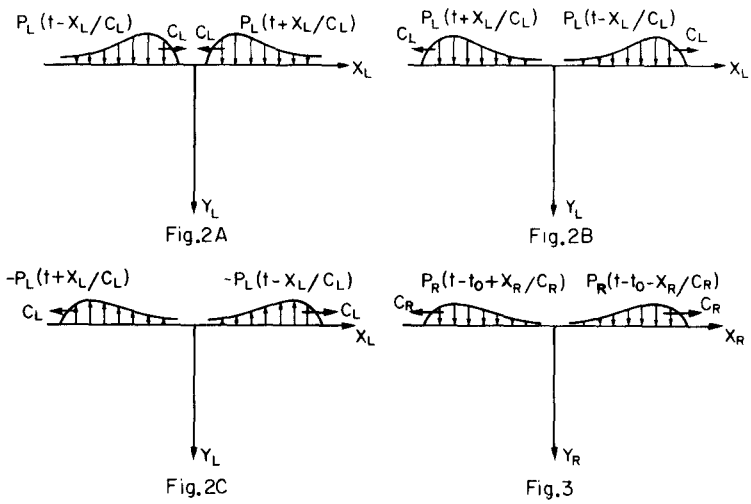

FIG. 2. Half-space problem equivalent to left-hand quarter-space problem of Fig. 1. (A) Equivalent steady-state problem for $-\infty < t < 0$. (B) Continuation of Fig. 2A with $t > 0$. (C) Transient portion of problem with $t > 0$.

FIG. 3. Transient half-space problem equivalent to right-hand quarter-space problem of Fig. 1 ($t > t_0$).

Throughout, xy are the coordinates for the original problem (Fig. 1), and x_Ly_L and x_Ry_R are the coordinates for the half-space models in Figs. 2 and 3, respectively. The y_L axis in Figs. 2 corresponds to the left side of the wall, while the y_R-axis in Fig. 3 represents the right side of the wall.

3.1 *Response in left-hand quarter-space*

Consider the half-space shown in Fig. 2A for $t < 0$ and in Fig. 2B for $t > 0$. It is subjected to the following two pressure wave loads on its surface:

$$\tau_{yy}(x_L, 0, t) = -p_L(t - x_L/c_L) - p_L(t + x_L/c_L); \qquad -\infty < x_L < \infty, \quad -\infty < t < \infty \tag{8a}$$

$$\tau_{xy}(x_L, 0, t) = 0; \qquad -\infty < x_L < \infty, \quad -\infty < t < \infty \tag{8b}$$

Now, the first term on the right side of equation (8a) is the same pressure wave traveling over the left-hand quarter-space in Fig. 1 [equation (6a)], and hence it produces in the left half of the half-space the same elastic waves which impinge on the left side of the wall in Fig. 1. The second term in (8a) is the "image" load and, since it travels in the negative x_L-direction, faster than the elastic waves, it produces no disturbances in the left half of the half-space for $t < 0$. For $t > 0$, however, it produces in the left half of the half-space *some* of the waves which are scattered by the left side of the wall. Note that we say "some" because, for $t > 0$, the image load in (8a) is moving over the left side of the half-space as shown in Fig. 2B; and no such load occurs on the left quarter-space of Fig. 1. Therefore, to determine the total scattered wave field in the left quarter-space, we must superimpose

the response in the left half of the half-space loaded as shown in Fig. 2C, i.e.,

$$\begin{aligned}\tau_{yy}(x_L, 0, t) &= p_L(t+x_L/c_L); \qquad x_L < 0, t > 0\\ \tau_{yy}(x_L, 0, t) &= p_L(t-x_L/c_L); \qquad x_L > 0, t > 0\end{aligned} \tag{9a}$$

$$\tau_{xy}(x_L, 0, t) = 0; \qquad -\infty < x_L < \infty, t > 0 \tag{9b}$$

to the response in the left half of the half-space in Fig. 2B. Note that the loading in (9) cancels the undesired effects of the image pressure wave in (8a). Zero initial conditions are also specified for the half-space problem in Fig. 2C because the total response must be continuous at $t = 0$.

For convenience we shall treat the half-space problems in Figs. 2A,B and in Fig. 2C separately, denoting the solutions with subscripts, AB and C, respectively.

For the problem in Figs. 2A,B with boundary conditions (8), recall that both the actual load, $p_L(t-x_L/c_L)$, and hence its image, $p_L(t+x_L/c_L)$, occur originally at $x_L \to \mp\infty$, respectively, and $t = 0$ is defined as that instant when these loads reach $x_L = 0$. Thus, for all finite values of time, the response to these loads will be quasi-static, depending only on the variables $(t \mp x_L/c_L)$ and y_L. The solution to this problem is obtained by the method with which Cole and Huth [4] determined the steady quasi-static response of a half-space subjected to a single, moving, concentrated, line load ($p_L(t) = \delta(t)$, where $\delta(t)$ is the Dirac delta function). Since this method is also discussed in detail in Fung's text [5], it is only outlined here and then the results are given.

Solutions of the equations of motion are taken in the form of outgoing plane compressional (P) and shear (S) waves produced by the two loads in (8a):

$$\begin{aligned}\phi_{AB}(x_L, y_L, t) &= \psi[t-(x_L+\alpha y_L)/c_L] + \psi[t+(x_L-\alpha y_L)/c_L]\\ h_{AB}(x_L, y_L, t) &= \sigma[t-(x_L+\beta y_L)/c_L] - \sigma[t+(x_L-\beta y_L)/c_L]\end{aligned} \tag{10}$$

where

$$\alpha = (c_L^2/c_1^2 - 1)^{\frac{1}{2}}, \qquad \beta = (c_L^2/c_2^2 - 1)^{\frac{1}{2}} \tag{11}$$

are real positive numbers, since $c_L > c_1 > c_2$. The first terms on the right of equations (10) represent the actual incident waves as shown in Fig. 1. Upon substituting these expressions into equations (3), (4), and then into the boundary conditions (8), we obtain the results:

$$\begin{aligned}\mu\ddot{\psi}(t) &= -c_L^2(\beta^2-1)Np_L(t)\\ \mu\ddot{\sigma}(t) &= 2\alpha c_L^2 Np_L(t); \qquad N = [(\beta^2-1)^2 + 4\alpha\beta]^{-1}\end{aligned} \tag{12}$$

where dots indicate differentiation with respect to time and it should be recalled that $p_L(t) \equiv 0$ for $t \leq 0$. This completes the solution of the problem in Figs. 2A,B. To calculate the reactions it produces on the left side of the wall, we substitute (10) with (12) into (4) to obtain

$$\begin{aligned}\tau_{xx}(0, y_L, t)|_{AB} &= 0; \qquad -\infty < t < \alpha y_L/c_L\\ \tau_{xx}(0, y_L, t)|_{AB} &= 2N(\beta^2-1)(2\alpha^2-\beta^2-1)p_L(t-\alpha y_L/c_L); \qquad \alpha y_L/c_L < t < \beta y_L/c_L\\ \tau_{xx}(0, y_L, t)|_{AB} &= 2N[(\beta^2-1)(2\alpha^2-\beta^2-1)p_L(t-\alpha y_L/c_L)\\ &\quad + 4\alpha\beta p_L(t-\beta y_L/c_L)]; \qquad \beta y_L/c_L < t\end{aligned} \tag{13}$$

Thus, the effects of the plane incident and reflected P waves, $\psi[t-(\alpha y_L \pm x_L)/c_L]$, respectively, are seen to occur initially at the left side of the wall at $t = \alpha y_L/c_L$, while the plane incident and reflected S waves, $\sigma[t-(\alpha y_L \pm x_L)/c_L]$, first arrive at $t = \beta y_L/c_L$. Of course, we must still superimpose the results from the problem in Fig. 2C to determine the total stress distribution along the left side of the wall.

To solve that problem (Fig. 2C) we follow the procedure used by Ang [6] who considered a half-space with a moving, concentrated, line load which started from rest. Again, this technique is explained in Fung's text [5] and so it is only briefly discussed here.

Since this is an initial value problem, we cannot use the steady, quasi-static solution in (10). Instead we begin the analysis by applying a Laplace transform in time and a Fourier transform in x_L to the equations of elastodynamics (1)–(4) and the boundary conditions (9), where

$$\bar{f}(x_L, y_L, s) = \int_0^\infty f(x_L, y_L, t)\, e^{-st}\, dt \tag{14a}$$

defines the Laplace transform of $f(x_L, y_L, t)$ and

$$\tilde{f}(\xi, y_L, t) = \int_{-\infty}^{\infty} f(x_L, y_L, t)\, e^{-i\xi x_L}\, dx_L \tag{14b}$$

is its Fourier transform.

The transformed boundary conditions (9) become

$$\begin{aligned} &\tilde{\bar{\tau}}_{yy}(\xi, 0, s) = 2s_L(\xi^2 + s_L^2)^{-1}\bar{p}_L(s); \qquad s_L = s/c_L \\ &\tilde{\bar{\tau}}_{xy}(\xi, 0, s) = 0 \end{aligned} \tag{15}$$

and it can be shown that solutions of the transformed equations of motion (1) which vanish as $y_L \to \infty$ and satisfy (15) are

$$\begin{aligned} \mu\tilde{\bar{\phi}}_c(\xi, y_L, s) &= (2\xi^2 + s_2^2)\Delta^{-1}\tilde{\bar{\tau}}_{yy}(\xi, 0, s)\, e^{-my_L} \\ \mu\tilde{\bar{h}}_c(\xi, y_L, s) &= 2im\xi\Delta^{-1}\tilde{\bar{\tau}}_{yy}(\xi, 0, s)\, e^{-ny_L} \end{aligned} \tag{16}$$

where

$$m^2 = \xi^2 + s_1^2, \qquad n^2 = \xi^2 + s_2^2, \qquad s_1 = s/c_1, \qquad s_2 = s/c_2 \tag{17}$$

and

$$\Delta(\xi, s) = (2\xi^2 + s_2^2)^2 - 4mn\xi^2 \tag{18}$$

is Rayleigh's function which vanishes only at $\xi = \pm is/\gamma$, γ being the velocity of Rayleigh waves in the half space. For real elastic materials, $0{\cdot}87 < \gamma/c_2 < 0{\cdot}96$.

The inversion of the transformed solution (16) throughout the half-space (Fig. 2C) can be accomplished with Cagniard's method [5, 6]. Briefly, this method consists of appropriately changing the integration variable in the Fourier transform inversion integral,

$$\bar{f}(x_L, y_L, s) = (2\pi)^{-1}\int_{-\infty}^{\infty} \tilde{\bar{f}}(\xi, y_L, s)\, e^{i\xi x_L}\, d\xi \tag{19}$$

so that the integral becomes the Laplace transform (14a) of some function of time (and position). Then the inverse Laplace transform operation yields that function.

Here, Cagniard's method will be used to determine the normal stress, $\tau_{xx}|_c$, along the y_L-axis. Substituting (16) into the transform of (4) and then into (19), we find

$$\bar{\tau}_{xx}(0, y_L, s)|_c = \mu\pi^{-1}\int_0^\infty [(s_2^2 - 2s_1^2 - 2\xi^2)\tilde{\bar{\phi}}(\xi, y_L, s) - 2in\xi\tilde{\bar{h}}(\xi, y_L, s)]\,d\xi \tag{20}$$

where we have used the fact that $\tilde{\tau}_{xx}$ is an even function of ξ to halve the range of integration from (19) to (20). To change (20) to a Laplace transform type integral, let $st = my_L$ and ny_L in the integrals involving $\tilde{\bar{\phi}}$ and $\tilde{\bar{h}}$, respectively, to obtain:

$$\bar{\tau}_{xx}(0, y_L, s)|_c = A_L y_L^{-1}\bar{p}_L(s)\left[\int_{y_L/c_1}^\infty P_L(t, y_L)\,e^{-st}\,dt + \int_{y_L/c_2}^\infty S_L(t, y_L)\,e^{-st}\,dt\right] \tag{21}$$

where

$$P_L = 0 \quad \text{for} \quad t < y_L/c_1,$$

$$P_L = \eta(2\eta^2 - 1)(2\eta^2 + \delta_2)\{(\eta^2 - \varepsilon^2)^{\frac{1}{2}}(\eta^2 - \varepsilon^2 + \kappa_L^2)[(2\eta^2 + \delta_2)^2 - 4\eta(\eta^2 - \varepsilon^2)(\eta^2 + \delta_1)^{\frac{1}{2}}\}^{-1} \quad \text{for} \quad t > y_L/c_1,$$

$$S_L = 0 \quad \text{for} \quad t < y_L/c_2$$

and

$$S_L = -4\eta^2[(\eta^2 - 1)(\eta^2 - \delta_1)]^{\frac{1}{2}}\{(\eta^2 - 1 + \kappa_L^2)[(2\eta^2 - 1)^2 - 4\eta(\eta^2 - 1)(\eta^2 - \delta_1)^{\frac{1}{2}}]\}^{-1} \tag{22}$$

for

$$t > y_L/c_2$$

are associated with the non-planar, transient, compressional and shear waves, respectively, which are scattered along the left side of the wall. In (21) and (22)

$$\eta = c_2 t/y_L, \quad \kappa_L = c_2/c_L, \quad \delta_1 = 1 - \varepsilon^2, \quad \delta_2 = 1 - 2\varepsilon^2,$$
$$A_L = -2\kappa_L c_2/\pi, \quad \text{and} \quad \varepsilon^2 = c_2^2/c_1^2 = (1 - 2\nu)/(2 - 2\nu). \tag{23}$$

Now, $\bar{\tau}_{xx}(0, y_L, s)|_c$ is expressed as the sum of two Laplace transforms of known functions. Therefore, we immediately can invert equation (21) as

$$\begin{aligned}
&\tau_{xx}(0, y_L, t)|_c = 0; && 0 < t < y_L/c_1\\
&\tau_{xx}(0, y_L, t)|_c = A_L y_L^{-1} p_L(t) * P_L(t, y_L); && y_L/c_1 < t < y_L/c_2\\
&\tau_{xx}(0, y_L, t)|_c = A_L y_L^{-1} p_L(t) * [P_L(t, y_L) + S_L(t, y_L)]; && y_L/c_2 < t
\end{aligned} \tag{24}$$

where

$$f(t)*g(t) \equiv \int_0^t f(\lambda)g(t-\lambda)\,d\lambda \tag{25}$$

denotes the convolution of $f(t)$ and $g(t)$.

The total stress distribution along the left side of the wall is the sum of (13) and (24). From it the resultant normal force, $F_L(t)$, and moment, $M_{OL}(t)$, can be calculated.

$$F_L(t) = -\int_0^\infty \tau_{xx}(0, y_L, t)\,dy_L, \qquad M_{OL}(t) = \int_0^\infty y_L \tau_{xx}(0, y_L, t)\,dy_L \tag{26}$$

where a positive force acts in the positive x-direction and a positive moment has a clockwise sense. The moment in (26) acts at the top of the wall, $y_L = 0$. To find the moment at an arbitrary point on the wall, $y_L = a$, we use

$$M_{aL}(t) = M_{OL}(t) + aF_L(t). \tag{27}$$

Substituting (13) in (26) we find

$$\begin{aligned} F_L(t)\|_{AB} &= 2c_2\delta_2(\alpha\kappa_L^5)^{-1}N[p_L(t)*1] \\ M_{OL}(t)\|_{AB} &= -2c_2^2(\alpha\beta\kappa_L)^{-2}[\delta_1 N(\beta^2-1)\kappa_L^{-4} - \alpha^2][p_L(t)*t] \end{aligned} \tag{28}$$

where α and β are defined in (11); N in (12); and κ_L, δ_1, and δ_2 in (23).

Similarly, we could substitute (24) into (26), but it is easier instead to calculate $F_L(t)\|_c$ and $M_{OL}(t)\|_c$ by performing the integration over y_L indicated in (26) directly on the expression for $\bar{\tau}_{xx}$ in (20). In this manner we obtain

$$\begin{aligned} \bar{F}_L(s)\|_c &= -2\delta_2\kappa_L\pi^{-1}s_2^5\bar{p}_L(s)\int_0^\infty \frac{d\xi}{\Delta(\xi, s)(\xi^2+s_1^2)^{\frac{1}{2}}(\xi^2+s_L^2)} \\ \bar{M}_{OL}(s)\|_c &= -2\kappa_L\pi^{-1}s_2\bar{p}_L(s)\left[\int_0^\infty \frac{d\xi}{(\xi^2+s_2^2)(\xi^2+s_L^2)}\right. \\ &\quad \left. -\delta_1 s_2^4\int_0^\infty \frac{(2\xi^2+s_2^2)\,d\xi}{\Delta(\xi, s)(\xi^2+s_1^2)(\xi^2+s_2^2)(\xi^2+s_L^2)}\right] \end{aligned} \tag{29}$$

where $\Delta(\xi, s)$ is defined in (18). The above expressions are readily inverted, for if ξ is replaced by $s_2\xi$ in the integrals in (29), $\bar{F}_L(s)\|_c$ and $\bar{M}_{OL}(s)\|_c$ are seen to be proportional to $\bar{p}_L(s)/s$ and $\bar{p}_L(s)/s^2$, respectively. Hence, it follows that

$$\begin{aligned} F_L(t)\|_c &= -2c_2\delta_2\kappa_L\pi^{-1}I_L[p_L(t)*1] \\ M_{OL}(t)\|_c &= -2c_2^2\kappa_L\pi^{-1}\{[2\kappa_L(\kappa_L+1)]^{-1}\pi - \delta_1 J_L\}[p_L(t)*t] \end{aligned} \tag{30}$$

where

$$\begin{aligned} I_L &= \int_0^\infty [(\xi^2+\varepsilon^2)^{\frac{1}{2}}(\xi^2+\kappa_L^2)\Omega(\xi)]^{-1}\,d\xi \\ J_L &= \int_0^\infty (2\xi^2+1)[(\xi^2+\varepsilon^2)(\xi^2+1)(\xi^2+\kappa_L^2)\Omega(\xi)]^{-1}\,d\xi \end{aligned} \tag{31}$$

with $\Omega(\xi) = (2\xi^2+1)^2 - 4\xi^2[(\xi^2+\varepsilon^2)(\xi^2+1)]^{\frac{1}{2}}$. Since $\Omega(\xi)$ vanishes only at $\xi = \pm ic_2/\gamma$ ($0{\cdot}87 < \gamma/c_2 < 0{\cdot}96$ for actual materials) the above integrals are convergent and, in fact, can be evaluated in terms of familiar, tabulated functions (see Appendix).

Thus, the total normal force on the left side of the wall

$$F_L(t) = F_L(t)|_{AB} + F_L(t)|_c \tag{32}$$

is proportional to the convolution of the intensity of the moving load and unity, whereas the total moment exerted at the top of the wall,

$$M_{OL}(t) = M_{OL}(t)|_{AB} + M_{OL}(t)|_c \tag{33}$$

is proportional to the intensity of the load convolved with t.

Numerical results for (32) and (33) are shown in Figs. 4. These will be discussed along with similar results for the reactions on the right side of the wall after the problem for the right-hand quarter-space is treated.

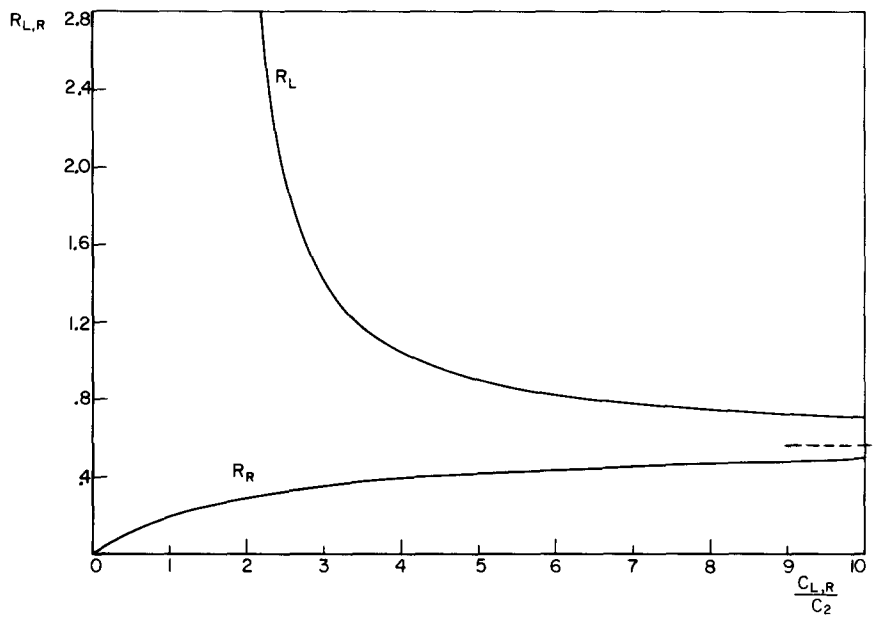

FIG. 4. Coefficients for the force on the left and right-hand sides of the wall vs. c_L/c_2 and c_R/c_2, respectively ($\nu = 0{\cdot}25$).

3.2 *Response in right-hand quarter-space*

Recalling that the pressure wave in Fig. 1 reaches the right side of the wall at $t = t_0$ and that its intensity and velocity then become $p_R(t)$ and c_R, respectively, we consider the half-space in Fig. 3 which is undisturbed for $t \leq t_0$ and which is subjected to the moving loads.

$$\begin{aligned} \tau_{yy}(x_R, 0, t) &= -p_R(t - t_0 - x_R/c_R); \qquad x_R > 0 \\ \tau_{yy}(x_R, 0, t) &= -p_R(t - t_0 + x_R/c_R); \qquad x_R < 0 \\ \tau_{xy}(x_R, 0, t) &= 0; \qquad -\infty < x_R < \infty \end{aligned} \tag{34}$$

for $t > t_0$. The load moving over the right half of the half-space ($x_R > 0$) is the same one specified in the original problem [eq. (6b)], while the load moving in the opposite direction over the left half ($x_R < 0$) is the image load. Therefore, boundary conditions (5) for the sides of the rigid-smooth wall will be satisfied along the y_R-axis in Fig. 3 and the response in the right half of this half-space will be equal to the response in the right quarter-space in Fig. 1.

The problem in Fig. 3 with boundary conditions (34) is very similar to the previously considered problem in Fig. 2C with boundary conditions (9). In fact, if t is replaced by $t-t_0$; x_L, y_L, and c_L by x_R, y_R, and c_R; and p_L by $-p_R$ in the latter problem, then we have exactly the problem in Fig. 3. Therefore, the solution of the right-hand quarter-space problem is readily determined from the solution in the right half of the half-space in Fig. 2C by observing the aforementioned changes. In particular, the normal stress along the right side of the wall follows from equations (24) as

$$\begin{aligned}
\tau_{xx}(0, y_R, t) &= 0; && 0 < t-t_0 < y_R/c_1 \\
\tau_{xx}(0, y_R, t) &= -A_R y_R^{-1}[p_R(t-t_0)*P_R(t, y_R)]; && y_R/c_1 < t-t_0 < y_R/c_2 \\
\tau_{xx}(0, y_R, t) &= -A_R y_R^{-1}\{p_R(t-t_0)*[P_R(t, y_R)+S_R(t, y_R)]\} && y_R/c_2 < t-t_0
\end{aligned} \tag{35}$$

where P_R and S_R are determined from (22) by changing $\kappa_L = c_2/c_L$ to $\kappa_R = c_2/c_R$ and $\eta = c_2 t/y_L$ to $\bar{\eta} = c_2(t-t_0)/y_R$. Also, $A_R = -2\kappa_R c_2/\pi$ and $*$ denotes the convolution operation defined in equation (25). In evaluating the resultant normal force and moment we must remember that a positive stress along the right side of the wall acts in the same direction as a positive force on this side. Hence,

$$F_R(t) = \int_0^\infty \tau_{xx}(0, y_R, t)\, dy_R; \qquad M_{OR}(t) = -\int_0^\infty y_R \tau_{xx}(0, y_R, t)\, dy_R \tag{36}$$

and the results follow from (30) as

$$\begin{aligned}
F_R(t) &= -2c_2\delta_2\kappa_R\pi^{-1} I_R[p_R(t-t_0)*1] \\
M_{OR}(t) &= -2c_2^2\kappa_R\pi^{-1}\{[2\kappa_R(\kappa_R+1)]^{-1}\pi - \delta_1 J_R\}[p_R(t-t_0)*t]
\end{aligned} \tag{37}$$

where I_R and J_R are found from (31) with κ_L replaced by κ_R.

3.3 *Numerical results for reactions on wall*

The total reactions on the left and right sides of the wall are given by the sum of equations (28) and (30) and by equation (37), respectively. It is observed that these results have the form

$$\begin{aligned}
F_L(t) &= c_2 R_L[p_L(t)*1], \qquad M_{OL}(t) = -c_2^2 B_L[p_L(t)*t] \\
F_R(t) &= -c_2 R_R[p_R(t-t_0)*1], \qquad M_{OR}(t) = c_2^2 B_R[p_R(t-t_0)*t]
\end{aligned} \tag{38}$$

where $R_{L,R}$ and $B_{L,R}$ are positive coefficients which depend only on $c_2/c_1 = \varepsilon$ (equation 2) and $c_2/c_{L,R} = \kappa_{L,R}$. These coefficients have been calculated numerically for a Poisson's ratio of the half-space, $\nu = 0{\cdot}25$, so that $\varepsilon = (3)^{-\frac{1}{2}}$. Figure 4 shows the variation of $R_{L,R}$ with $c_{L,R}/c_2$ while similar curves are presented in Fig. 5 for $B_{L,R}$.

It is seen from both figures that the reactions on the left side of the wall become infinite as $c_L \to c_1 = 3^{\frac{1}{2}}c_2$. (Recall that the analysis of the problem in the left quarter-space is

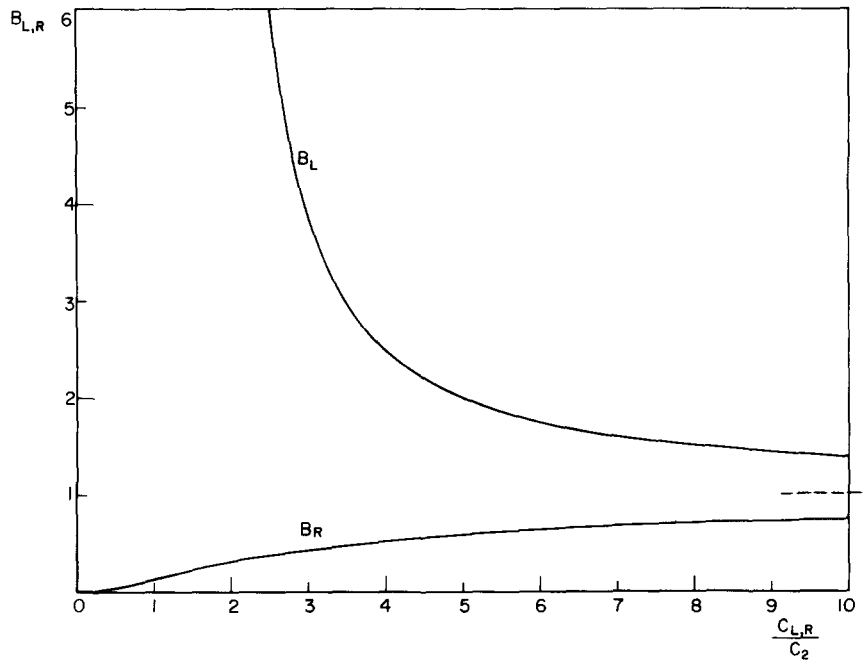

FIG. 5. Coefficients for the moment at the top of the left and right sides of the wall vs. c_L/c_2 and c_R/c_2, respectively ($\nu = 0{\cdot}25$).

valid only for $c_L > c_1$.) This is due to the factor $\alpha^{-1} = [(c_L/c_1)^2 - 1]^{-\frac{1}{2}}$ in equations (28) and can be accounted for physically from Fig. 1 and equations (10). As $c_L \to c_1$, the incident plane P wave front becomes parallel to the wall, i.e., $\phi_{AB} \to \psi(t - x_L/c_2)$. In such a case the wall would be subjected to a uniform normal stress over its entire left surface which in turn would produce an infinite force and moment on the wall. Both coefficients, R_L and B_L, decrease monotonically as c_L increases, with $R_L \to (3)^{-\frac{1}{2}}$ and $B_L \to 1$ as $c_L \to \infty$. These limits are indicated on the figures.

The coefficients for the reactions on the right side of the wall are zero for $c_R = 0$ since this would imply that the right-hand quarter-space is never subjected to load. As c_R increases, these coefficients increase and also approach the limits, $R_R \to (3)^{-\frac{1}{2}}$ and $B_R \to 1$ as $c_R \to \infty$. This does not mean, however, that the net reactions on the wall $(F_L + F_R, M_{OL} + M_{OR})$ become zero as $c_{L,R} \to \infty$, for, although $t_0 \to 0$, $p_R(t)$ still need not be equal to $p_L(t)$.

4. SUMMARY AND CONCLUSIONS

The problem of the dynamic loading of a rigid-smooth wall which divides an elastic half-space into two quarter-spaces has been studied for the case of an arbitrary plane, moving, pressure wave load on the surface. Since the boundary conditions along a rigid-smooth vertical boundary of a quarter-space are identically satisfied along the y-axis of a half-space subjected to symmetric loading, exact solutions for the present problem can be determined. The major results presented are the reactions occurring on the wall. For the

infinitely long wall (in the y-direction of Fig. 1) considered here, these results are valid for all times. Furthermore, such a wall has infinite mass so that its rigid body motion is always zero.

Nevertheless, the results of this study may also be applied in the case of a finite wall for times, $t < \alpha l/c_L$, where l is the length of the wall. This is because $t = \alpha l/c_L$ is the time when the front of the incident compressional wave (equation 10) would reach the bottom of the left side of the wall. The time when the front of the compressional wave would reach the bottom of the right side is $t = t_0 + l/c_1$ which is larger than $\alpha l/c_L$ since $\alpha < c_L/c_1$. Therefore, the reactions on a finite wall, held fixed, are correctly given by equations (38) for $t < \alpha l/c_L$. To determine the subsequent rigid-body motion of a finite wall, one can use the rigid-fixed reactions given here for $t < \alpha l/c_L$ as "forcing functions" after the "transfer function" or free vibration solution is known. This method of splitting the reactions on a rigid mobile inclusion into rigid-fixed and free vibration portions is discussed in a previous work [7].

Acknowledgements—This research was sponsored by Bell Telephone Laboratories, Whippany, New Jersey. The author appreciates the support and encouragement of Drs. Ashley Carter and Frank Flaherty. Also, the author wishes to thank Dr. James Dally of Illinois Institute of Technology for his useful suggestions in the course of this work.

REFERENCES

[1] S. A. THAU and Y. H. PAO, Diffractions of horizontal shear waves by a parabolic cylinder and dynamic stress concentrations. *J. appl. Mech.* **33**, 785–792 (1966).
[2] C. C. MOW and J. W. WORKMAN, Dynamic stresses around a fluid filled cavity. *J. appl. Mech.* **33**, 793–799 (1966).
[3] J. MIKLOWITZ, Elastic wave propagation. *Applied Mechanics Surveys*, pp. 809–839. Spartan (1966).
[4] J. COLE and J. HUTH, Stresses produced in a half-plane by moving loads. *J. appl. Mech.* **25**, 433–436 (1958).
[5] Y. C. FUNG, *Foundations of Solid Mechanics*, pp. 218–225, 259–268. Prentice-Hall (1965).
[6] D. D. ANG, Transient motion of a line load on the surface of an elastic half-space. *Q. appl. math.* **18**, 251–256 (1960).
[7] S. A. THAU, Radiation and scattering from a rigid inclusion in an elastic medium. *J. appl. Mech.* **34**, 509–511 (1967).
[8] *Handb. Mathematical Functions*, edited by M. ABRAMOWITZ and I. A. STEGUN, pp. 587–626. Dover (1965).

APPENDIX

Expressions for the coefficients, $R_{L,R}$ and $B_{L,R}$, appearing in equations (38) contain the integrals, $I_{L,R}$ and $J_{L,R}$, respectively, which are defined in equations (31) and immediately following equation (37). Dropping the subscripts L,R we have

$$I = \int_0^\infty [(\xi^2 + \tfrac{1}{3})^{\frac{1}{2}}(\xi^2 + \kappa^2)\Omega(\xi)]^{-1}\, d\xi$$
$$J = \int_0^\infty (2\xi^2 + 1)[(\xi^2 + \tfrac{1}{3})(\xi^2 + 1)(\xi^2 + \kappa^2)\Omega(\xi)]^{-1}\, d\xi \tag{39}$$

$$\Omega(\xi) = (2\xi^2 + 1)^2 - 4\xi^2[(\xi^2 + \tfrac{1}{3})(\xi^2 + 1)]^{\frac{1}{2}} \tag{40}$$

when Poisson's ratio is 0·25. Rationalizing the denominators in (39) we obtain

$$I = \frac{3}{8}\left\{\int_0^\infty (\xi^2 + \tfrac{1}{3})^{-\frac{1}{2}} f_1(\xi)\, d\xi + \int_0^\infty (\xi^2 + 1)^{-\frac{1}{2}} f_2(\xi)\, d\xi\right\}$$
$$J = \frac{3}{4}\left\{\int_0^\infty f_3(\xi)\, d\xi + \int_0^\infty [(\xi^2 + \tfrac{1}{3})(\xi^2 + 1)]^{-\frac{1}{2}} f_4(\xi)\, d\xi\right. \tag{41}$$

where

$$f_1(\xi) = (\xi^2+\tfrac{1}{2})^2[(\xi^2+\kappa^2)(\xi^2+\tfrac{1}{4})(\xi^2+a_+^2)(\xi^2+a_-^2)]^{-1}$$
$$f_2(\xi) = \xi^2(\xi^2+1)(\xi^2+\tfrac{1}{2})^{-2} f_1(\xi)$$
$$f_3(\xi) = (\xi^2+\tfrac{1}{2})[(\xi^2+\tfrac{1}{3})(\xi^2+1)]^{-1} f_1(\xi)$$
$$f_4(\xi) = \xi^2(\xi^2+\tfrac{1}{2})^{-1} f_1(\xi) \tag{42}$$

and

$$a_\pm^2 = (3 \pm 3^{\frac{1}{2}})/4. \tag{43}$$

Each of the above functions, $f_i(\xi)$, can be expressed as a sum of partial fractions of the form $C/(\xi^2+b^2)$ where C and $b^2 > 0$ are constants. The details are lengthy, but straightforward and we are left with four different types of integrals. In the expression for I we must integrate terms of the form

$$I_i = \int_0^\infty [(\xi^2+r_i^2)^{\frac{1}{2}}(\xi^2+b^2)]^{-1}\,\mathrm{d}\xi; \qquad (r_1 = \tfrac{1}{3}, r_2 = 1) \tag{44a}$$

and in J we have integrals of the form

$$J_1 = \int_0^\infty (\xi^2+b^2)^{-1}\,\mathrm{d}\xi \tag{44b}$$

$$J_2 = \int_0^\infty [(\xi^2+\tfrac{1}{3})(\xi^2+1)]^{-\frac{1}{2}}(\xi^2+b^2)^{-1}\,\mathrm{d}\xi \tag{44c}$$

Making the substitutions $\xi = r_i x(1-x^2)^{-\frac{1}{2}}$, $\xi = b\tan x$, and $\xi = 3^{-\frac{1}{2}}\tan x$ in 44a, b, and c, respectively, we obtain

$$\begin{aligned} I_i &= \int_0^1 [b^2+(r_i^2-b^2)x^2]^{-1}\,\mathrm{d}x \\ &= [b(r_i^2-b^2)^{\frac{1}{2}}]^{-1}\tan^{-1}[(r_i^2-b^2)^{\frac{1}{2}}/b]; && b^2 < r_i^2 \\ &= r_i^{-2}; && b^2 = r_i^2 \\ &= [b(b^2-r_i^2)^{\frac{1}{2}}]^{-1}\ln\left[\frac{b}{r_i}+\left(\frac{b^2}{r_i^2}-1\right)^{\frac{1}{2}}\right]; && b^2 > r_i^2 \end{aligned} \tag{45a}$$

$$J_1 = b^{-1}\int_0^{\pi/2} \mathrm{d}\theta = \pi/2b \tag{45b}$$

$$\begin{aligned} J_2 &= (b^2-\tfrac{1}{3})^{-1}\left\{\int_0^{\pi/2}(1-\tfrac{2}{3}\sin^2 x)^{-\frac{1}{2}}\right\}\mathrm{d}x \\ &\quad -(3b^2)^{-1}\int_0^{\pi/2}\{(1-\tfrac{2}{3}\sin^2 x)^{\frac{1}{2}}[1-(1-(3b^2)^{-1})\sin^2 x]\}^{-1}\,\mathrm{d}x \\ &= (b^2-\tfrac{1}{3})^{-1}\{K(\tfrac{2}{3})-(3b^2)^{-1}\Pi[(1-(3b^2)^{-1});\pi/2;\sin^{-1}(\tfrac{2}{3})]\} \end{aligned} \tag{45c}$$

In (45c), $K(\frac{2}{3})$ is the complete elliptic integral of the first kind with parameter, $\frac{2}{3}$; and Π is the elliptic integral of the third kind with parameter, $\frac{2}{3}$, amplitude, $\pi/2$, and characteristic, $[1-(3b^2)^{-1}]$ [8].

Therefore, in the manner just outlined, we can obtain explicit expressions for I and J in terms of tabulated functions [8].

(*Received* 11 *April* 1967; *revised* 3 *July* 1967)

Абстракт—В работе исследуется динамические силы действующие вдоль сторон жесткой и гладкой стены, которая разделяет упругое полупространство на две четверти пространства. Край полупространства находится под влиянием волны давления, произвольной формы, движущейся с постоянной скоростью. Форма и скорость волны могут изменятся при переходе сквозь стены. Решаются точно две задачи для каждой четверти полупространства, используя метод отображений в связи с выведенным ранее анализом для динамических задач полупространства. Даются в явной форме результаты для суммарной силы и момента, вызыванных на стене. Эти реакции являются пропорциональными свертке истории нагрузки, относительно с единицей и иовремеиц. Выведено численно константы пропорциональности для широкого круга скоростей волны давления.